Chapter 2
Laser Diode Beam Basics

Abstract The basic properties of single transverse mode and multi-transverse mode laser diode beams are reviewed. The characteristics of a laser diode beam propagating through optical elements is analyzed using three commonly used math tools: analytical tool thin lens equation and ABCD matrix, numerical calculation, and software tool Zemax. The emphasis is on using thin lens equation and numerical calculation to study the collimation and focusing characteristics of single transverse mode laser diode beams.

Keywords Astigmatism · Beam · Beam waist · Collimation · Divergence · Elliptical · Fast axis · Focal length · Focus · Gaussian · Image distance · Lens · M^2 factor · Object distance · Propagation · Rayleigh range · Raytracing · Slow axis · Spot size · Transverse mode

Single transverse mode laser diodes are most widely used. Their beams are elliptical, astigmatic, and have large divergence. These characteristics make laser diode beams difficult to handle. In this chapter we discuss in detail the basics of laser diode beams mainly using a simple paraxial Gaussian model. This model is accurate enough for most applications.

Multi-transverse laser diode beams are not typical laser beams and are also discussed in this chapter.

2.1 Single Transverse Mode Laser Diode Beams

2.1.1 Elliptical Beams

When a laser diode is operated, a portion of the laser field will transmit through one facet of the active layer and becomes the emitted laser beam. Because the active layer of a laser diode has a rectangular shaped cross section and a portion of the laser field will leak out from the active layer due to the limited confinement, the beam at the emission facet is a little larger than the cross section of the active layer

H. Sun, *A Practical Guide to Handling Laser Diode Beams*,
SpringerBriefs in Physics, DOI 10.1007/978-94-017-9783-2_2

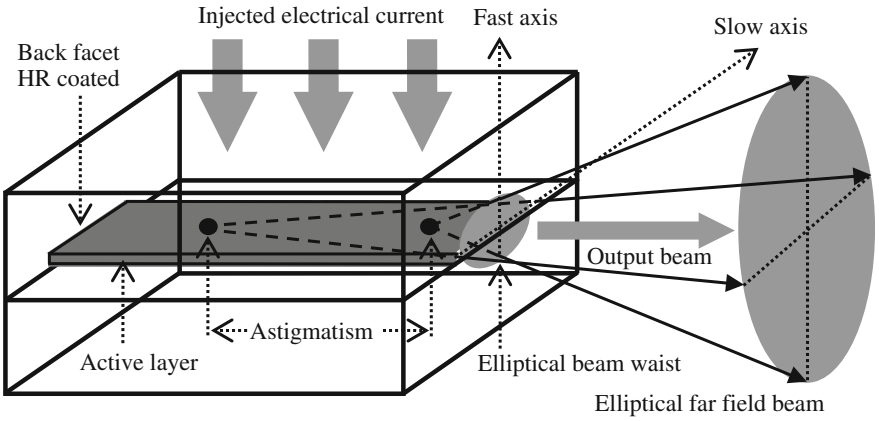

Fig. 2.1 A laser diode has a thin active layer. The emitted laser beam shown is *elliptical*, highly divergent, and astigmatic. The astigmatism magnitude is much exaggerated for clarity

and has an elliptical shape, as shown in Fig. 2.1. The beam size at the emission facet is about one micron in the direction vertical to the active layer and a few microns in the direction horizontal to the active layer. The beam elliptical ratio is typically from 1:2 to 1:4. The beam far field divergence is also different in the vertical and horizontal directions with a typical ratio of 2:1–4:1. Because the beam divergence is larger in the vertical direction, this direction is often called the "fast axis" direction. Then, the horizontal direction is called "slow axis" direction, as shown in Fig. 2.1.

As the beam propagates, the beam size in the fast axis direction will surpass the beam size in the slow axis direction, because the beam divergence is larger in the fast axis direction. The beam shape will become vertically elliptical, as shown in Fig. 2.1. This phenomenon is unique to laser diode beams. An elliptical shape beam is one of the undesired characteristics of laser diodes.

2.1.2 Large Divergences

The divergence of single transverse (TE) mode laser diode beams can vary significantly from different types of laser diodes and can even vary from diode to diode of the same type. The typical full width half magnitude (FWHM) divergent angle is about 15°–40° and 6°–12° in the fast and slow axis directions, respectively. In terms of $1/e^2$ intensity divergence, this is about 26°–68° and 10°–20° in the fast and slow axis directions, respectively. The laser diode industry traditionally uses the FWHM divergent angle to specify the beam divergence, because the FWHM number is more consistent; while in the optical community, the $1/e^2$ intensity divergence is often used. The latter is about 1.7 times larger than the former.

Because of the very large divergence in the fast axis direction, the lens used to collimate or focus a laser diode beam must have at least one aspheric surface to correct the spherical aberration and a numerical aperture (NA) of at least 0.3 to avoid severe beam truncation, although a lens with an NA of 0.6 will still truncate some beams. Most aspheric lenses specially designed and fabricated for collimating laser diode beams available in the market have an NA ranging from 0.3 to 0.6. Truncation of a beam will create side lobes, cause focal shift to the beam, and increase the divergence of the beam. The large divergent beam is another undesired characteristic of laser diodes.

2.1.3 Quasi-Gaussian Intensity Profiles

The spatial shape o of a laser diode beam is determined by the structure of the active layer. As described in Chap. 1, the active layer is one rectangular shaped waveguide or several rectangular shaped waveguides in parallel. TE modes of such active layers are not exactly Gaussian modes. The gain inside the active layer and the loss outside the active layer will also affect the mode shapes. There are many different active layer structures. The TE modes from these active layers are slightly different. There is no single mathematical model that can accurately describe all these modes and no commonly accepted relationship linking laser diode types to the shapes of their TE modes. Only individual case studies have been reported [1–3]. Based on this author's experience, in most practical applications the differences among most single TE modes of various types of laser diodes are insignificant and all these modes can be described with negligible error by a Gaussian model, since the Gaussian model is the simplest and most widely used model.

If we need be more specific, most single TE mode laser diode beams have slightly narrower central lobe and slightly longer tails compared with Gaussian mode.

2.1.4 Astigmatism

Laser diode beams are astigmatic; this is a consequence of the rectangular shaped active layer and the varying gain profile across the active layer in the slow axis direction. As shown in Fig. 2.1, the waist of a laser beam in the fast axis direction is located near the facet of the active layer, while the beam waist in the slow axis direction is located somewhere behind, that is, the astigmatism. The astigmatism depicted in Fig. 2.1 is much exaggerated for clarity. Similar to other laser diode parameters, astigmatism magnitude varies from different types of laser diodes and from diode to diode of the same type. For single TE mode laser diodes, the astigmatism is usually from 3 to 10 μm. For multi-TE mode laser diodes, the astigmatism is usually from 10 to 50 μm. From the application point of view, there

is no need to study the origin of the astigmatism. We are more interested in measuring and correcting the astigmatism.

An astigmatic beam is another undesired characteristic of single TE mode laser diodes.

2.1.5 Polarization

Laser diode beams are linear polarized. The polarization ratio is high from about 50:1 to about 100:1 for single TE mode laser diode, and around 30:1 for wide stripe multi-TE modes laser diodes. The polarization is in the slow axis direction. The high polarization ratio of laser diode beams can be either an advantage or a disadvantage, depending on the type of applications. As a comparison, most He–Ne laser beams are randomly polarized.

2.2 Multi-transverse Mode Laser Diode Beams

2.2.1 Wide Stripe Laser Diode Beams

More carriers and photons are needed to increase the laser power. This can be achieved by increasing the volume of the active layer. However, as discussed in Chap. 1, high lasing efficiency requires high carrier density inside the active layer. This means the active layer thickness cannot be increased. Then, the straightforward way to increase the laser power is to increase the active layer width. For laser diodes with power higher than 100 mW or so (depending on the laser diode type and wavelength), the active layer widths are tens of microns or even up to a few hundred microns. Such laser diodes are often called wide stripe laser diodes or broad area laser diodes. The beam emitted from a wide stripe active layer contains multiple TE modes as depicted in Fig. 2.2. Every TE mode is a quasi-Gaussian mode. All these modes combine to form a multi-TE mode beam. As the beam

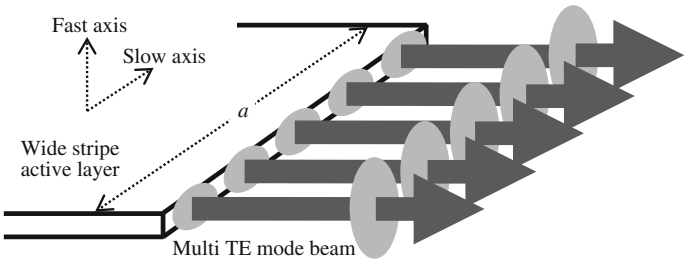

Fig. 2.2 The beam of a wide stripe laser diode contains multiple TE modes

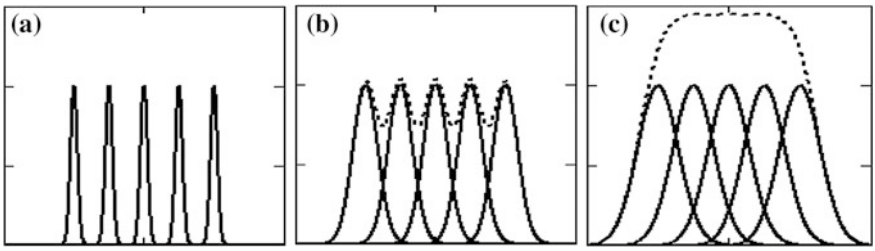

Fig. 2.3 The *solid curves* are for the spatial intensity distributions of five TE modes at three propagations distances. **a** At or near the diode facet. **b** At ten microns or so from the laser diode facet. **c** At tens of microns or beyond. The *dashed curves* are the spatial intensity distribution of five modes combined. The horizontal axis is spatial distance in the slow axis direction with a scale of tens of microns. The vertical axis is intensity with arbitrary unit

propagates, every mode increases its size and gradually merges with other modes to form a light line in the slow axis direction, as shown in Fig. 2.2. As the beam further propagates, the beam shape becomes rectangular, because all the modes have larger divergence in the fast axis direction.

Figure 2.3 shows the spatial intensity distribution of five TE modes at three different propagation distances. Figure 2.3a shows the intensity distribution of the five modes at or near the laser diode facet. As the beam propagates, the sizes of the five modes increase, the modes gradually merge together as shown in Fig. 2.3b, c by the thin curves. The intensity distributions of the five modes combined are shown in Fig. 2.3b, c by the dashed curves. When we scan such a multi-TE mode beam, the scan head is usually at least several millimeters away from the laser diode, the scan result will be something similar to that shown by the dashed curve in Fig. 2.3c. However, such a beam is not a true flat top beam. When the beam is focused, the intensity profile of the focused spot will be as shown in Fig. 2.3a if the focusing lens is of high quality, or like that shown by the dashed curve in Fig. 2.3b, where if the focusing lens has large aberration it will increase the size of the focused modes.

The beams of wide stripe laser diodes are not like the laser beams we have often seen, but are somehow like the lights from a light bulb. These beams cannot be well collimated or focused to small spots. We will discuss this in detail in Sect. 3.8.

2.2.2 Laser Diode Stack Beams

Several wide stripe active layers can be stacked up to further increase the laser power. Such a laser is called laser diode stack. There are many different combinations of active layer widths and stack layers. Figure 2.4 shows the schematic of a four-layer laser diode stack. There are many TE modes in the beam. The power of a laser diode stack can be up to thousands of watts. A laser diode stack can be treated

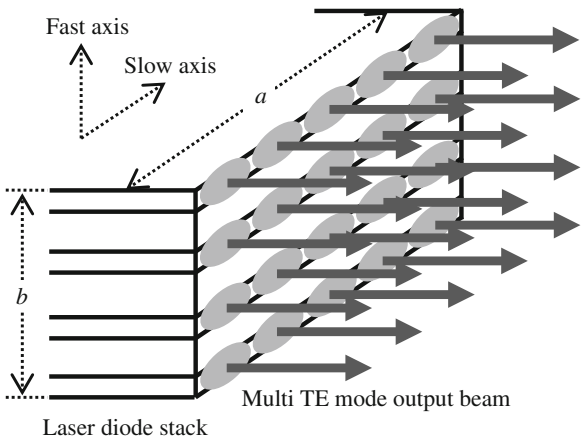

Fig. 2.4 Schematic of a laser diode stack

as a rectangular shaped light source of size $a \times b$ as shown in Fig. 2.4. The beams of laser diode stacks are not like the laser beams we often see, but are rather like the lights from a flashlight. These beams cannot be well collimated or focused to small spots. We will discuss this in detail in Sect. 3.8.

2.3 Laser Diode Beam Propagation

2.3.1 Basic Mode Paraxial Gaussian Beams

Most laser beams have a circular shaped cross section with a Gaussian intensity profile. Such beams are basic TE mode Gaussian beams. The characteristics of a Gaussian beam can be described by a set of three equations [4]

$$w(z) = w_0 \left[1 + \left(\frac{M^2 \lambda z}{\pi {w_0}^2} \right)^2 \right]^{1/2} \tag{2.1}$$

$$R(z) = z \left[1 + \left(\frac{\pi {w_0}^2}{M^2 \lambda z} \right)^2 \right] \tag{2.2}$$

$$I(r, z) = I_0(z) \mathrm{e}^{-2r^2/w(z)^2} \tag{2.3}$$

where $w(z)$ is the $1/\mathrm{e}^2$ intensity radius of the beam at z, z is the axial distance from the waist of the laser beam, w_0 is the $1/\mathrm{e}^2$ intensity radius of the beam waist, M^2 is the M square factor, λ is the wavelength, $R(z)$ is the beam wavefront curvature radius at z, $I(r, z)$ is the beam intensity radial distribution in a cross section plane at z, r is the radial coordinate in a cross section plane at z, and $I_0(z)$ is the beam peak

intensity in a cross section plane at z. The M square factor $M^2 \geq 1$ describes the deviation of the beam from a perfect Gaussian beam. For a perfect laser beam $M^2 = 1$. We will discuss the M^2 factor in detail in Sect. 2.3.2.

For a laser beam the Rayleigh range z_R is defined as that at $z = z_R$ the beam radius is $w(z_R) = \sqrt{2}\, w_0$. From Eq. (2.1) we can see that

$$z_R = \frac{\pi {w_0}^2}{M^2 \lambda} \tag{2.4}$$

z_R is proportional to ${w_0}^2$. From Eq. (2.1) we can also see that at far field, z is large, term $M^2\lambda z/\pi {w_0}^2 = z/z_R \gg 1$, the $1/e^2$ intensity far field half divergent angle θ of the beam can be obtained by

$$\begin{aligned} \theta &= \frac{w(z)}{z} \\ &= \frac{M^2 \lambda}{\pi w_0} \\ &= \frac{w_0}{z_R} \end{aligned} \tag{2.5}$$

θ is inversely proportional to the beam waist w_0. Figure 2.5 plots Eq. (2.1) for two Gaussian laser beams with $w_0 = 1$ mm and $w_0 = 0.5$ mm, respectively. The far field divergence θ_1 and θ_2 define the asymptote lines for the two beams, respectively. z_{R1} and z_{R2} of the two laser beams are marked in Fig. 2.5.

Figure 2.6 plots Eq. (2.2) for two laser beams same as the two beams in Fig. 2.5. It can be seen from Eq. (2.2) and Fig. 2.6 that at the beam waist, both beams have a

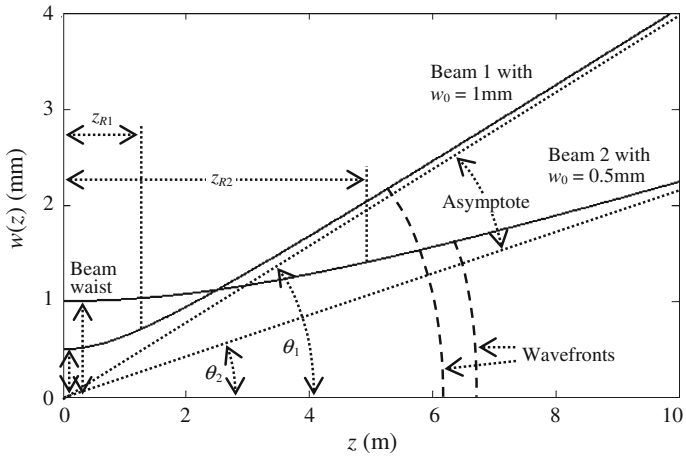

Fig. 2.5 The *solid curves* are $w(z)$ versus z for two laser beams with w_0 = 1.0 and 0.5 mm, respectively, both beams have λ = 0.635 μm and M^2 = 1

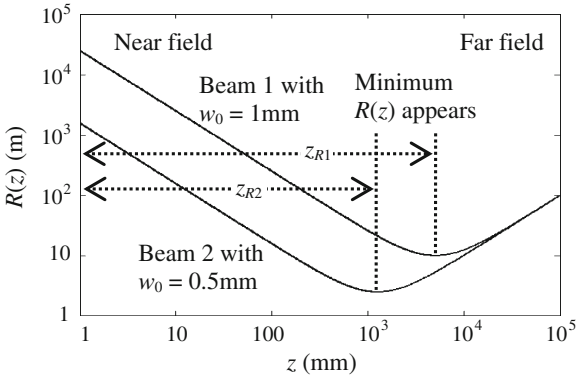

Fig. 2.6 $R(z)$ versus z for two laser beams with $w_0 = 1.0$ and 0.5 mm, respectively, $\lambda = 0.635$ μm and $M^2 = 1$

plane wavefront with radius $R(0)$ approaching infinity. As the beam propagates, $R(z)$ gradually decreases. The minimum $R(z)$ appears at $z = z_R$. As the beam continues propagating, the beam wavefront gradually becomes spherical, then $R(z)$ becomes proportional to z. z_R is often used as a criterion, $z \ll z_R$ is "near field", $z \gg z_R$ is "far field", and $z \sim z_R$ is the intermediate field.

Figure 2.7 plots Eq. (2.3) for a laser beam with Gaussian intensity distribution in an arbitrary cross section perpendicular to the propagation direction of the beam, where $I_0(z)$ is normalized to 1. Beam radius is usually defined at either $1/e^2$ intensity level or at FWHM level. We can find from Eq. (2.3) that the $1/e^2$ intensity radius equals $w(z)$, and the half magnitude radius equals $0.59w(z)$. The ratio between these two radii is about 1.7.

The percentage of laser energy encircled inside the $1/e^2$ intensity radius can be calculated by

$$\frac{\int_0^{w(z)} e^{-2r^2/w(z)^2} r dr}{\int_0^{\infty} e^{-2r^2/w(z)^2} r dr} = 86.4\,\% \tag{2.6}$$

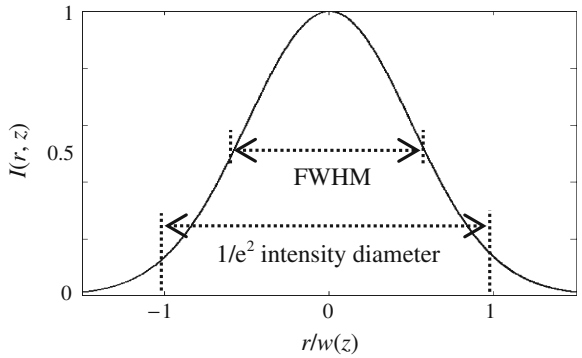

Fig. 2.7 Normalized Gaussian intensity distribution

where r is the radial variable. Similarly, the percentage laser energy encircled inside the half magnitude radius can be calculated by

$$\frac{\int_0^{0.59w(z)} e^{-2r^2/w(z)^2} r dr}{\int_0^{\infty} e^{-2r^2/w(z)^2} r dr} = 69.2\,\%. \tag{2.7}$$

The characteristics of basic TE mode Gaussian beams have been studied extensively. Many works studying this subject have been published. The most cited one is probably the book *Lasers* written by Siegmann [5].

2.3.2 M^2 Factor Approximation

The beams of some solid state lasers and laser diodes are not exact basic mode Gaussian beams, they may contain higher order Gaussian modes. It is difficult to find the mode structure details in these beams, since the unavoidable measurement errors often lead to inconclusive results. A practical way of handling such laser beams is to neglect the mode structure details, assume the beams still have Gaussian intensity distributions, and introduce a M^2 factor to the beams [6, 7]. By definition, $M^2 = 1$ means the beam is a perfect basic mode Gaussian beam. $M^2 \geq 1$ means the beam deviates from a basic mode Gaussian beam.

Figures 2.8 and 2.9 plot Eqs. (2.1) and (2.2) for two beams with the same waist size and wavelength, but different $M^2 = 1$ and 1.2, respectively. We can see that the beam far field divergence is proportional to the value of the M^2 factor. Most collimated single TE mode laser diode beams have a M^2 of 1.1 and 1.2. The introduction of the M^2 factor enables the equation set for basic mode Gaussian beam to describe non-basic mode Gaussian with reasonable accuracy and thereby significantly simplify the mathematics involved. M^2 factor has been widely used now to describe various quasi-Gaussian laser beams. Some laser developers even use M^2 factor to

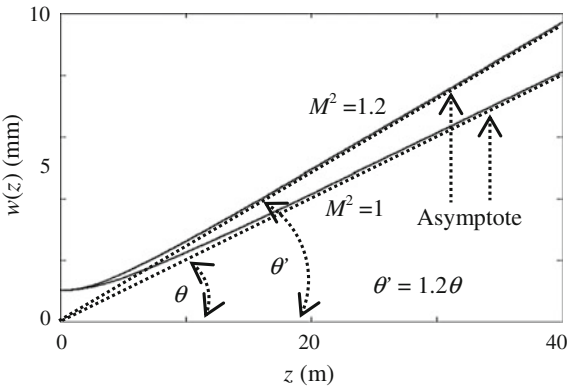

Fig. 2.8 *Solid curves* are $w(z)$ versus z for two laser beams with $M^2 = 1$ and 1.2, respectively. Both beams have $w_0 = 1.0$ mm and $\lambda = 0.635$ μm

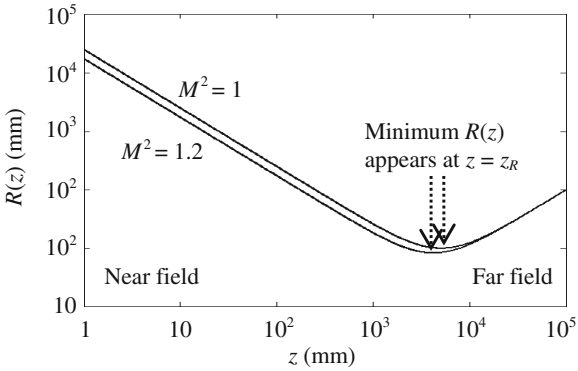

Fig. 2.9 *Solid curves* are $R(z)$ versus z for two laser beams with $w_0 = 1.0$ mm, $\lambda = 0.635$ mm, and $M^2 = 1$ and 1.2, respectively

describe multi-TE mode laser beams. ISO has established a detail procedure for measuring M^2 factor [8].

2.3.3 Thin Lens Equation for a Real Laser Beam

Thin lens equation was originally derived as a simple analytical model to describe how a lens manipulates geometric rays. Thin lens equation is an approximated model, but accurate enough in most applications, and is therefore widely used. Thin lens equation has the form [9]

$$\frac{i}{f} = \frac{o}{o - f} \tag{2.8}$$

where o is the object distance measured from the object point to the lens principal plane. The lens focuses the rays from the object point and produces an image of the object point, i is the image distance measured from the image point to the lens principal plane, and f is the focal length of the lens. The lens magnification ratio m is defined as

$$m = \frac{i}{o} \tag{2.9}$$

Equation (2.8) shows that for $o = f_+$, $i \to \infty$ and $m \to \infty$, the rays are collimated, where f_+ means a value slightly larger than f. For $o = f_-$, $i \to -\infty$ and $m \to -\infty$, the rays are also collimated, where f_- means a value slightly smaller than f. For $o \to \infty$, $i \to f$ and $m \to 0$, the rays are focused. It is noted that the geometric optics is not accurate to calculate the size of a focused spot, the actual smallest possible focused spot radius is the diffraction limited radius $1.22\lambda f/d$, where d is the ray bundle diameter.

Equation (2.8) was first modified to be applicable to a basic mode Gaussian beam without considering the M^2 factor [10] and was later expanded to include the M^2 factor [4]. The latest form of thin lens equation looks like

$$\frac{i}{f} = \frac{\frac{o}{f}\left(\frac{o}{f} - 1\right) + \left(\frac{z_R}{f}\right)^2}{\left(\frac{o}{f} - 1\right)^2 + \left(\frac{z_R}{f}\right)^2} \tag{2.10}$$

where o is the object distance measured from the waist of the laser beam incident on the lens to the principal plane of the lens, i is the image distance measured from the waist of the laser beam output from the lens to the principal plane of the lens, and z_R is the incoming Rayleigh range of the incident beam defined in Eq. (2.4). The M^2 factor is included in z_R. z_R/f is an important parameter in Eq. (2.10). For $z_R/f \rightarrow 0$, Eq. (2.10) reduces to Eq. (2.8), which means such a laser beam can be treated as geometric rays emitted by a point source. For $z_R/f \rightarrow \infty$, Eq. (2.10) leads to $i = f$, the laser beam is focused at the focal point of the lens.

Equation (2.10) has some interesting characteristics that are different from those of Eq. (2.8). One characteristics is the maximum and minimum focusing distance that can be found by differentiating Eq. (2.10) and assuming $\Delta i/\Delta o = 0$, we obtain

$$o = f \pm z_R \tag{2.11}$$

Plugging $o = f + z_R$ into Eq. (2.10), we can find the maximum focusing distance to be

$$i_{max} = f\frac{\frac{2z_R}{f} + 1}{\frac{2z_R}{f}} \tag{2.12}$$

Plugging $o = f - z_R$ into Eq. (2.10) we can find the minimum focusing distance to be

$$i_{min} = f\frac{\frac{2z_R}{f} - 1}{\frac{2z_R}{f}} \tag{2.13}$$

z_R/f again plays an important role here. For $z_R/f \gg 1$, Eqs. (2.12) and (2.13) reduce to $i_{\max} = i_{\min} = f$, which is a focusing situation. For $z_R/f \ll 1$, Eqs. (2.12) and (2.13) reduce to $i_{\max} \rightarrow \infty$ and $i_{\min} \rightarrow -\infty$, the beam is collimated similar to collimated geometric rays emitted by a point source.

For a typical laser diode beam, z_R is several microns; assuming this laser diode beam is collimated by a lens with a focal length of several millimeters, we have $z_R/f \sim 0.001$, Eq. (2.12) reduces to $i_{\max} \approx f^2/2z_R \approx 500f \sim 1$ m, and Eq. (2.13) reduces to $i_{\min} \approx -f^2/2z_R \approx -500f \sim -1$ m. The negative value of $i_{\min}$ indicates that

the laser beam outgoing from the lens has an imaginary waist on the left-hand side of the collimation lens.

The waist of a collimated laser diode beam is a few millimeters, the z_R of such a collimated beam is several meters. When this collimated laser diode beam is focused by a lens with a focal length of several millimeters, we have $z_R/f \sim 1000$, Eqs. (2.12) and (2.13) give $i_{max} \approx 1.001f$ and $i_{min} \approx 0.999f$, respectively. This means the position of the focused spot of the beam can shift around the lens focal point in the range of ~ 1 μm.

Equations (2.10) and (2.8) are plotted in Fig. 2.10 by solid and dashed curves, respectively, with z_R/f = 0.1, 0.2, 0.4 and 1, respectively. The maximum and minimum focusing distances i_{max} and i_{min} are marked by the open circles and open squares on each curve. Figure 2.10 shows that for $o/f = 1$, $i/f = 1$ for any z_R/f values. For smaller z_R/f, i changes faster as o changes and the values of i_{max} and $|i_{min}|$ are larger. When $z_R/f \rightarrow 0$, the Gaussian beam reduces to a point source, the solid curve approaches the dashed curve.

The magnification of a lens on a laser beam propagating through the lens is defined by the ratio of w_0'/w_0, where w_0' is the waist radius of the beam output from the lens. w_0'/w_0 can be found by modifying Eq. (2.9) as [4].

$$m = \frac{w_0'}{w_0} = \frac{1}{\left[\left(\frac{o}{f} - 1\right)^2 + \left(\frac{z_R}{f}\right)^2\right]^{0.5}} \tag{2.14}$$

The M^2 factor is included in z_R as defined in Eq. (2.4). $w_0'/w_0 \gg 1$ indicates the beam is collimated. $w_0'/w_0 \ll 1$ indicates the beam is focused. $w_0'/w_0 \sim 1$ means

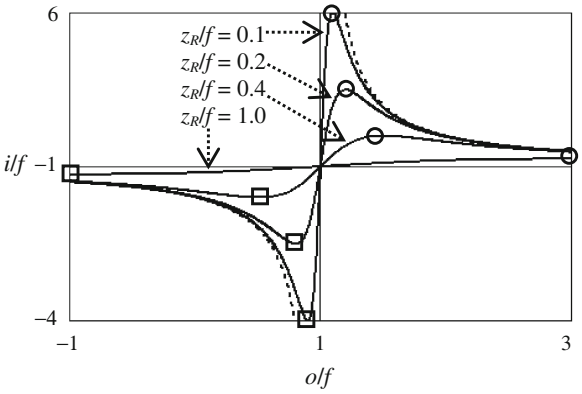

Fig. 2.10 The *solid curves* are i/f versus o/f curves with z_R/f = 0.1, 0.2, 0.4 and 1, respectively. The *dashed curves* plotted here for comparison are for geometric rays emitted by a point source. i_{max} and i_{min} are marked by the *open circles* and *open squares* on each curve

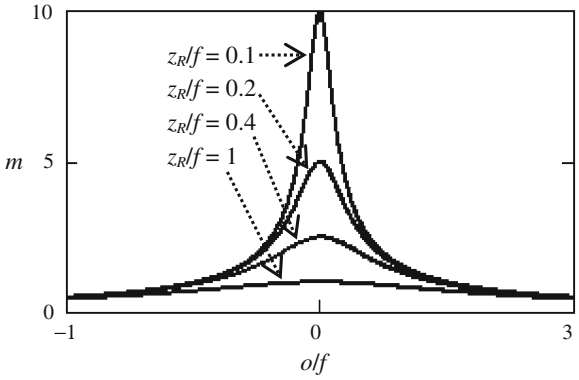

Fig. 2.11 Lens magnification m versus o/f curve with z_R/f being a parameter

the beam is relayed. From Eq. (2.14) we can see that $w_0'/w_0 = 1$ can appear for various combinations of o/f and z_R/f. It can be seen that for $z_R/f \rightarrow 0$, the Gaussian beam reduces to a point source and Eq. (2.14) reduces to Eq. (2.9).

Equation (2.14) is plotted in Fig. 2.11 with z_R/f being a parameter. We can see from Fig. 2.11 that for any z_R/f values, m peaks at $o/f = 1$. For $o/f = 1$, m is larger for smaller z_R/f, since this is a collimation situation, a smaller waist size incident beam means larger divergence and larger waist size of collimated beam. For $z_R/f > 1$, the value of m does not change much as the value of o/f changes, since this is a focusing situation; the waist size of the focused spot does not change much when the incident beam waist location changes.

2.3.4 Non-paraxial Gaussian Beams

Laser beams with larger divergent angles can be non-paraxial Gaussian beams and cannot be treated accurately by the basic mode paraxial Gaussian model.

Nemoto [11] shows that when $ks_0 < 4$ the paraxial Gaussian model deviates appreciably from the exact solution and that when $ks_0 < 2$ the paraxial Gaussian model differs considerably from the exact solution, where s_0 is the 1/e intensity radius of the beam waist and $k = 2\pi/\lambda$ is the wave vector. s_0 can be converted to the more commonly used $1/e^2$ intensity radius w_0 of the beam waist by $s_0 = 0.368w_0$, then Nemoto's two conditions can be written, respectively, as

$$w_0 < 1.73\lambda \tag{2.15}$$

$$w_0 < 0.87\lambda \tag{2.16}$$

It would be difficult to directly measure the waist radius w_0 of an un-manipulated beam of laser diode, since the waist is at the emission facet and is likely only about 1 μm, but it would be much easier to measure the far field divergence of the

un-manipulated beam. Also, every datasheet of laser diode provides the far field FWHM divergence $2\theta_{\mathrm{FWHM}}$, not w_0. It will be more convenient to replace w_0 in Eqs. (2.15) and (2.16) by the far field divergence. The paraxial Gaussian model relates the $1/e^2$ intensity far field half divergence θ to w_0 by Eq. (2.5). We know that Eq. (2.5) itself is a paraxial approximation and we are now talking about the inaccuracy of paraxial Gaussian model. But it is still adequate to use Eq. (2.5) to provide a criterion for assessment. Combining Eqs. (2.5), (2.15), and (2.16) to eliminate w_0 and converting θ from radian to degree, we obtain two conditions in terms of degree

$$2\theta > 21^\circ \quad \text{or} \quad 2\theta_{\mathrm{FWHM}} > 12.4^\circ \tag{2.17}$$

for paraxial Gaussian model deviates appreciably from the exact solution and

$$2\theta > 42^\circ \quad \text{or} \quad 2\theta_{\mathrm{FWHM}} > 24.7^\circ \tag{2.18}$$

for paraxial Gaussian model considerably differs from the exact solution. Checking the datasheets of various laser diodes, we can find that the slow axis divergence of almost all laser diodes does not meet these two conditions, paraxial Gaussian model is accurate enough to treat laser diode beams in the slow axis direction, and that the fast axis divergence of many laser diodes meets Eq. (2.17) or even Eq. (2.18), which means many laser diode beam are non-paraxial in the fast axis direction. As we will show later in Sect. 3.2, if we can accept an error of 10 % or so, then the paraxial Gaussian model discussed in this chapter can still be used to treat laser diode beams in the fast axis direction. Otherwise, we have to use Kirchhoff diffraction integral to perform accurate numerical analysis.

Figure 2.12 shows the far field angular intensity distribution of a non-paraxial laser diode beam at 5 mm. The solid curve is accurate obtained using Kirchhoff

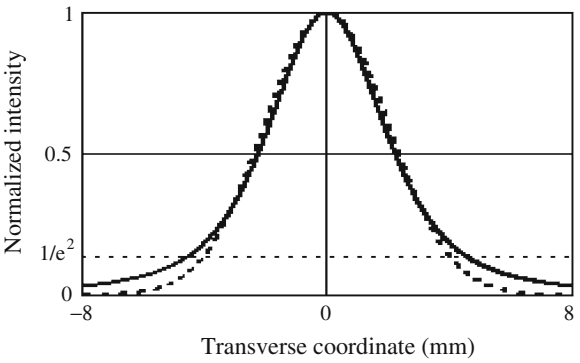

Fig. 2.12 Normalized intensity profiles at 5 mm for a non-paraxial Gaussian beam with a $1/e^2$ intensity radius of 0.25 μm and a wavelength of 0.635 μm. *Solid curve* is obtained using Kirchhoff diffraction integration. *Dashed curve* is obtained using paraxial Gaussian model

diffraction integration. The dashed curve is approximation obtained using paraxial Gaussian model. We will discuss the characteristics of non-paraxial Gaussian beam in detail in Sect. 3.2.

2.3.5 Raytracing Technique

2.3.5.1 ABCD Matrix Method

A geometric ray propagating through optical elements can be conveniently analyzed by ABCD matrix method [12]. Below we consider a simple example. As shown in Fig. 2.13a, a ray propagates from a medium with index n_1 to another medium with index n_2. The interface of these two media is planar. The input ray can be described by its height x_1 when it hits the optics surface and its angle θ_1 to the optical axis. Similarly, the output ray can be described by its height x_2 when it leaves the optics surface and its angle θ_2 to the optical axis. We have

$$x_2 = x_1 \tag{2.19}$$

$$\theta_2 = \frac{n_1}{n_2}\theta_1 \tag{2.20}$$

Equation (2.20) is the paraxial form of Snell's law [13]. We can write Eqs. (2.19) and (2.20) in the matrix form

$$\begin{aligned}\begin{bmatrix} x_2 \\ \theta_2 \end{bmatrix} &= \begin{bmatrix} A & B \\ C & D \end{bmatrix} \begin{bmatrix} x_1 \\ \theta \end{bmatrix} \\ &= \begin{bmatrix} 1 & 0 \\ 0 & \frac{n_1}{n_2} \end{bmatrix} \begin{bmatrix} x_1 \\ \theta_1 \end{bmatrix}\end{aligned} \tag{2.21}$$

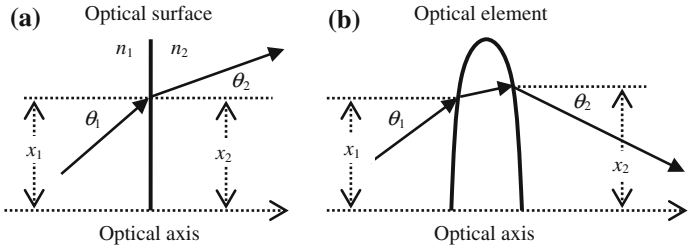

Fig. 2.13 **a** A geometric ray propagates through an optical surface. **b** A geometric ray propagates through a lens

Table 2.1 Commonly used ABCD matrix

Optical element	Matrix
Propagation in a uniform medium	$\begin{bmatrix} 1 & d \\ 0 & 1 \end{bmatrix}$
Refraction at a planar surface	$\begin{bmatrix} 1 & 0 \\ 0 & \frac{n_1}{n_2} \end{bmatrix}$
Refraction at a curved optical surface	$\begin{bmatrix} \frac{n_1 - n_2}{R \cdot n_2} & \frac{0}{n_1} \\ & \frac{n_2}{n_2} \end{bmatrix}$
Reflection from a planar mirror	$\begin{bmatrix} 1 & 0 \\ 0 & 1 \end{bmatrix}$
Reflection from a curved mirror	$\begin{bmatrix} 1 & 0 \\ \frac{2}{R} & 1 \end{bmatrix}$
Thin lens	$\begin{bmatrix} 1 & 0 \\ -\frac{1}{f} & 1 \end{bmatrix}$
Thick lens	$\begin{bmatrix} \frac{n_2 - n_1}{R_2 \cdot n_1} & \frac{0}{n_1} \\ & \frac{n_2}{n_2} \end{bmatrix} \begin{bmatrix} 1 & t \\ 0 & 1 \end{bmatrix} \begin{bmatrix} \frac{n_1 - n_2}{R_1 \cdot n_2} & \frac{0}{n_1} \\ & \frac{n_2}{n_2} \end{bmatrix}$

Equation (2.21) shows that an optical surface can be described by a 2×2 matrix. Figure 2.13b shows a more general case, a ray propagates through a lens, then x_2 is not necessary equal to x_1. If a geometric ray propagates through n optical elements, the height and angle of the output ray can be calculated by

$$\begin{bmatrix} x_n \\ \theta_n \end{bmatrix} = \begin{bmatrix} A_1 & B_1 \\ C_1 & D_1 \end{bmatrix} \cdots \begin{bmatrix} A_n & B_n \\ C_n & D_n \end{bmatrix} \begin{bmatrix} x_1 \\ \theta_1 \end{bmatrix} \tag{2.22}$$

Each matrix in Eq. (2.22) describes one optical surface. The process of solving Eq. (2.22) is much simpler than the process of exhaustively tracing the ray through every optical surface.

Reference [12] and many other optics text books provide a list of matrices for various commonly used optical elements. For readers' convenience, we re-produce with minor modifications a list here in Table 2.1. It is not difficult to prove these matrices. In the table, d is the axial distance, R is the radius of curvature, $R > 0$ for convex surface and $R < 0$ for concave surface, f is the focal length, $f > 0$ for positive lens and $f < 0$ for negative lens, and n_1 and n_2 are the initial and final refractive indexes, respectively. For the thick lens, t is the lens center thickness, n_1 and n_2 are the refractive indexes outside and inside the lens, respectively, and R_1 and R_2 are the radii of curvature of the first and second surfaces, respectively.

2.3.5.2 Apply ABCD Matrix to a Gaussian Beam

The ABCD matrix method was originally developed to analyze geometric rays propagating through optical elements. These rays in a uniform medium are straight lines. By definition, a ray propagates in the direction of wavefront normal. For a Gaussian beam, the wavefront radius and wavefront center positions change as the beam propagates, therefore the propagation direction of a "ray" in a Gaussian beam also changes.

To apply ABCD matrix method to analyze the propagation of a Gaussian beam, we need to conceive a ray in the beam and follow this ray through the optical element. Considering an example of a thin lens shown in Fig. 2.14, we can conceive an input ray and an output ray for the beam, the rays are the tangents of any intensity contours of the input and output beams at the lens, respectively. It is more convenient to conceive the rays at the $1/e^2$ intensity level. Because we already know the input beam data, we can find the $1/e^2$ intensity height $w(z)$ and the $1/e^2$ intensity divergent angle θ for the input ray, as shown in Fig. 2.14. Note that the lens is not necessary at the far field of the beam, θ here is not necessary for the far field divergent angle given by Eq. (2.5). Applying the ABCD matrix to the input ray, we have

$$\begin{bmatrix} w'(z) \\ \theta' \end{bmatrix} = \begin{bmatrix} 1 & 0 \\ -\frac{1}{f} & 1 \end{bmatrix} \begin{bmatrix} w(z) \\ \theta \end{bmatrix} \tag{2.23}$$

where $w'(z)$ and θ' are the $1/e^2$ intensity height and divergent angle for the output ray.

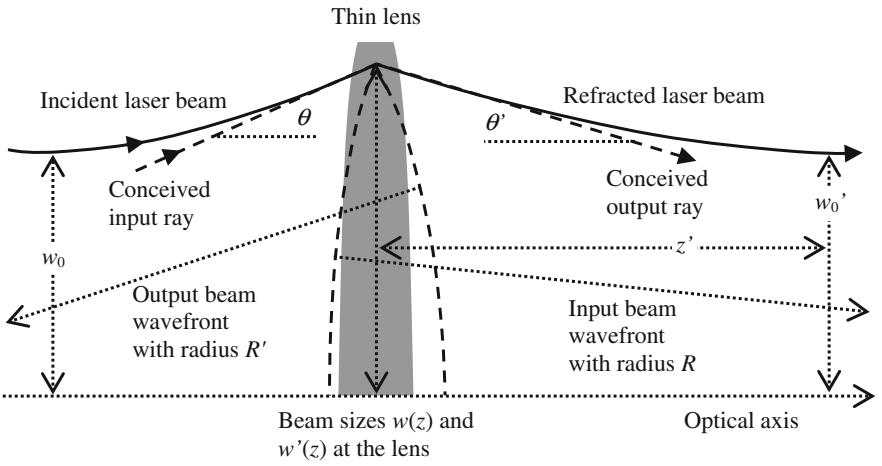

Fig. 2.14 A laser beam propagates through a thin lens

Solving Eq. (2.23), we obtain

$$w'(z) = w(z) \tag{2.24}$$

$$\theta' = -\frac{w(z)}{f} + \theta \tag{2.25}$$

Equation (2.24) is obvious, as can be seen in Fig. 2.14. We also have paraxial relations $\theta = w(z)/R$ and $\theta' = w'(z)/R'$, where R and R' are the wavefront radii of the input and output rays at the lens, respectively, as shown in Fig. 2.14, and R is known. Inserting the two relations into Eq. (2.25), we obtain R'

$$\frac{1}{R'} = \frac{1}{R} - \frac{1}{f} \tag{2.26}$$

Equation (2.26) is the same as the geometric thin lens equation.

Having obtained $w'(z)$ and R', we can back calculate the $1/e^2$ intensity waist radius $w_0{}'$ and waist location z' of the output beam by modifying Eqs. (2.1) and (2.2) to

$$w_0{}' = \frac{w'(x)}{\left[1 + \frac{w'(z)^4 \pi^2}{R'(z)^2 (M^2 \lambda)^2}\right]^{0.5}} \tag{2.27}$$

$$z' = \frac{R'(x)}{1 + \frac{R'(z)^2 (M^2 \lambda)^2}{w'(z)^4 \pi^2}} \tag{2.28}$$

The derivation of Eqs. (2.27) and (2.28) is a little complex, we write the main steps here. Equations (2.1) and (2.2) are rewritten here for readers' convenience.

$$w'(z) = w_0{}' \left[1 + \left(\frac{M^2 \lambda z'}{\pi w_0{}'^2}\right)\right]^{1/2} \tag{2.1}$$

$$R'(z) = z' \left[1 + \left(\frac{\pi w_0{}'^2}{M^2 \lambda z'}\right)\right] \tag{2.2}$$

Taking the square of both sides of Eq. (2.1) and dividing the result by Eq. (2.2), we obtain

$$\frac{w'(z)^2}{R'(z)} = \frac{w_0{}'^2 \left[1 + \left(\frac{M^2 \lambda z'}{\pi w_0{}'^2}\right)^2\right]}{z' \left[1 + \left(\frac{\pi w_0{}'^2}{M^2 \lambda z'}\right)^2\right]} \tag{2.29}$$

Taking the $(M^2\lambda z')^2/(\pi\ {w_0}'^2)^2$ term out of the parenthesis in the numerator of Eq. (2.29) and canceling the same terms in the numerator and denominator, Eq. (2.29) becomes

$$\begin{aligned}\frac{w'(z)^2}{R'(z)} &= \frac{{w_0}'^2\left(\frac{M^2\lambda z'}{\pi {w_0}'^2}\right)^2\left[1+\left(\frac{\pi {w_0}'^2}{M^2\lambda z'}\right)^2\right]}{z'\left[1+\left(\frac{\pi {w_0}'^2}{M^2\lambda z'}\right)^2\right]} \\ &= \frac{z'}{{w_0}'^2}\left(\frac{M^2\lambda}{\pi}\right)^2 \quad \text{or} \\ \frac{z'}{{w_0}'^2} &= \frac{w'(z)^2}{R'(z)}\left(\frac{\pi}{M^2\lambda}\right)^2\end{aligned} \tag{2.30}$$

Inserting Eq. (2.30) into the parentheses of Eqs. (2.1) and (2.2), and solving for ${w_0}'$ and z', respectively, we obtain Eqs. (2.27) and (2.28).

Reference [14] provides a detailed study on ray equivalent modeling of Gaussian beams.

2.4 Zemax Modeling of a Gaussian Beam Propagating Through a Lens

Zemax is probably the most widely used optical design software. Zemax can perform sequential raytracing for designing imaging optics and non-sequential raytracing for designing illumination optics. Zemax offers three editions with different capabilities and prices. The two higher editions, Professional and Premium editions, have the feature of modeling Gaussian beams propagating through optics, a useful tool that can save a lot time and effort when designing laser optics. Although in its 2014 manual, Zemax describes this feature in the ***Physical Optics*** section in Chapter 7, Analysis Menu and in Chapter 26, Physical Optics Propagation, this feature is still not well known to many users. In this section, we use two examples to demonstrate, step-by-step, how to use Zemax to model a Gaussian beam propagating through a lens. We assume the readers are already familiar with the geometric raytracing feature of Zemax and will emphasize the procedure difference between Zemax sequential raytracing and Gaussian beam modeling.

We use mm as the length unit throughout Sect. 2.4.

2.4.1 Collimating a Gaussian Beam

To start designing optics using Zemax sequential raytracing, the first three parameters to be selected are the *Field*, *General/Aperture,* and *Wavelength* in the

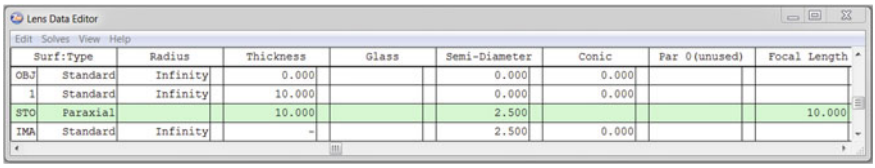

Fig. 2.15 Zemax *Lens Data Editor* for modeling a Gaussian beam propagating through a paraxial lens

System drop-down list. The first two parameters are irrelevant for modeling Gaussian beam, we randomly pick up 0° field and 5 mm aperture. We still need select wavelength since it is a parameter of Gaussian beam. Here we pick up 0.65 μm for the wavelength, just for demonstration purpose. Then we open the *Lens Data Editor* box. The thickness of the *OBJ* surface is important for sequential raytracing, but irrelevant again for modeling Gaussian beam, we type in 0 for simplicity. We select *Surface 2* as the *STP* surface and place an ideal *Paraxial* lens with 10 mm focal length at the *STO* surface. We type in 10 in the *Surface 1 Thickness* box, *Surface 1* is then 10 mm away from the *STO* surface and is at the focal plane of the lens. Type in 10 in the surface *STO Thickness* box, which means surface *IMA* is 10 mm away from surface *STO* and is at another focal plane of the lens. After typing in these data, the *Lens Data Editor* box will look like as shown in Fig. 2.15.

Then we need to set the parameters for the Gaussian beam to be modeled. Click *Analysis* button, in the drop-down list, click *Physical optics* button, there are four choices in the drop-down list: *Paraxial Gaussian beam*, *Skew Gaussian beam*, *Physical Optics Propagation*, and *Beam File Viewer*. Laser diode beams are skew (elliptical) Gaussian beams. But here we only model a paraxial (circular) Gaussian beam for simplicity. After we have mastered the modeling process, we can model the skew Gaussian beam feature without difficulties.

Click the *Paraxial Gaussian beam* button, a text box *Paraxial Gaussian Beam Data* appears, we will look at it later. Click the *Settings* button at the top of the text box, a table box *Paraxial Gaussian Beam Settings* appears. Then we can type in the parameters of the laser diode beam. In the table box, we have only one choice for the wavelength, that is, 0.65 μm selected by us earlier. Type 0.002 in *Waist size* box, which means the $1/e^2$ intensity waist (radius) of the embedded fundamental mode beam of the input beam is 0.002 mm. This small waist size is common for laser diodes and such a small beam has large divergence. An ideal Gaussian beam has $M^2 = 1$, here we type 1.2 in the M^2 *factor* box for a mixed mode beam. When modeling Gaussian beam, the object is the beam waist, the distance between the beam waist and surface 1 is defined by the value in the *Surf 1 to waist* box. When we type in 0, the beam waist is set at surface 1 and is at the focal plane of the paraxial lens, a negative value here means the beam waist is at the left side of the surface. Since the Rayleigh range of this beam is much smaller than the focal length of the lens, this is a collimating situation, as explained in Sect. 3.1.4. For a skew Gaussian beam, the beam behaves differently in the *x*-*z* and *y*-*z* planes. For a

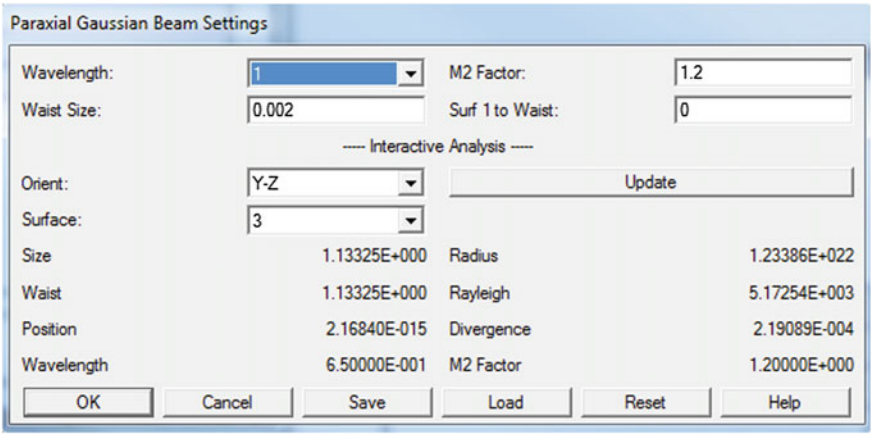

Fig. 2.16 Content of table box *Paraxial Beam Settings* after typing in all the data and clicking *Update*

circular Gaussian beam modeled here, the orientation does not matter, we randomly choose *Y-Z* in the *Orient* box. The number filled in the *Surface* box selects the surface at which the beam parameters will be shown in the table box; we select number 3 which is the last surface. We will see soon that the beam parameters at every surface will be shown later in the text box *Paraxial Gaussian Beam Data*. After typing in all these numbers, click the *Update* button in the table box, the table box will look like as shown in Fig. 2.16. The beam data shown in the lower half of the box is for surface 3. We do not explain these data now, since they will be shown in the text box again.

Click the *Update* button in the text box *Paraxial Gaussian Beam Data*, the relevant part of the text box will look like as shown in Fig. 2.17. In Zemax sequential raytracing, any one surface can be selected as *Global coordinate reference*, the positions of all other surfaces are relative to this surface. In Zemax Gaussian beam modeling, the beam waist position is relative to any surface that is under consideration. We need to keep this difference in mind when interpreting the modeling results shown in Fig. 2.17. We also note that all the beam data shown for a surface is AFTER the beam propagating through the surface.

Let us first check the beam data at every surface for the *Fundamental mode results* shown in Fig. 2.17. This results are for an ideal Gaussian beam with $M^2 = 1$ embedded in the beam we set with $M^2 = 1.2$.

OBJ surface. Since we let the distance between *OBJ* surface and surface *1* be 0, all the beam data in these two surfaces are the same.

Surface *1*:

(Beam) *Size* at this surface is 2.00000E−3. Because the beam waist we typed in is 0.002 mm and the waist is at this surface.

Waist (size) is 2.00000E−3, as we typed in earlier.

Input Beam Parameters:

Waist size : 2.00000E-003

Surf 1 to waist distance : 0.00000E+000

M Squared : 1.20000E+000

Y-Direction:

Fundamental mode results:

Sur	Size	Waist	Position	Radius	Divergence	Rayleigh
OBJ	2.00000E-000	2.00000E-003	0.00000E+000	Infinity	1.03084E-001	1.93329E-002
1	2.00000E-003	2.00000E-003	0.00000E+000	Infinity	1.03084E-001	1.93329E-002
STO	1.03451E+000	1.03451E+000	-1.00000E+001	-2.67552E+006	2.00000E-004	5.17254E+003
IMA	1.03451E+000	1.03451E+000	2.16840E-015	Infinity	2.00000E-004	5.17254E+003

Mixed Mode results for M2 = 1.2000:

Sur	Size	Waist	Position	Radius	Divergence	Rayleigh
OBJ	2.19089E-003	2.19089E-003	0.00000E+000	1.00000E+010	1.12923E-001	1.93329E-002
1	2.19089E-003	2.19089E-003	0.00000E+000	1.00000E+010	1.12923E-001	1.93329E-002
STO	1.13325E+000	1.13325E+000	-1.00000E+001	-2.67552E+006	2.19089E-004	5.17254E+003
IMA	1.13325E+000	1.13325E+000	2.16840E-015	1.23386E+022	2.19089E-004	5.17254E+003

Fig. 2.17 Zemax modeling of a paraxial lens collimating a Gaussian beam. Shown here is the content of the text box *Paraxial Gaussian beam Parameters*. Only the *Y-direction* content is pasted here, since the beam is circular; the *X-direction* content is the same and is neglected

(Beam waist) *Position* is 0.00000E+000, which means the distance between the beam waist and surface 1 is 0. This is what we typed in earlier.

Radius is infinity. Since the beam waist is at surface 1, the wavefront at surface 1 must be flat.

Divergence is 1.03084E−001. Note that the divergence is the far field divergence, not the divergence at this specific surface. For a given waist size, wavelength, and M^2 factor, there is only one far field divergence as given by Eq. (2.5), no matter what surface we are considering. Zemax calculated the divergence based on the beam parameters we type in.

Rayleigh (range) is 1.93329E–002. Again, for a given waist size, wavelength, and M^2 factor, there is only one Rayleigh range given by Eq. (2.4), no matter what surface we are considering. Zemax calculated the Rayleigh range based on the beam parameters we type in.

Surface *STO*

Since we put a paraxial lens at surface *STO* and the waist of the input beam is at the focal plane of the lens, the beam is collimated after it passes through surface *STO*.

(Beam) *Size* is 1.03451E+000 calculated by Zemax.
Waist (size) is 1.03451E+000 calculated by Zemax. Note that the waist of the collimated beam is at surface *IMA* as will be shown in the *Position* below, but the waist size and beam size at surface *STO* are virtually the same, because the beam is collimated and the two surfaces are only 10 mm apart.
(Beam waist) *Position* is −1.00000E+001, which means the waist of the collimated beam is 10 mm away from surface *STO*. The negative sign here indicates that the waist of the collimated beam is on the right side of surface *STO*.
Radius is −2.67552E+006, surface *STO* is only 10 mm away from surface *IMA* where the waist of the collimated beam is located. The wavefront radius at surface *STO* must be large.
Divergence is 2.00000E−4, very small, since the beam is collimated with a waist size of about 1 mm.
Rayleigh is 5.17254E+003 and should match the waist size of the collimated beam.

Surface *IMA*

The *Size* and *Waist* are the same as those at surface *STO*, since the beam is collimated and these two surfaces are only 10 mm apart. The beam waist *Position* is relative to surface *IMA* and is virtually 0. The positive sign means the beam waist position is slightly on the left-hand side of surface *IMA*. The *Radius* is infinity because the beam waist is at this surface.

Now, let us check the *Mixed Mode results for* $M^2 = 1.2000$ in Fig. 2.17. The *Position*, *Radius*, and *Rayleigh* are virtually the same as those for the *Fundamental mode*. The *Waist* of the input beam is about 1.2 times larger than the *Waist* of the embedded beam because we select $M^2 = 1.2$. The *Waist* and *Size* of the collimated beam are about 1.1 times larger than those of the embedded beam. The *Divergence* is about 1.1 times larger for every surface. The situation is illustrated in Fig. 2.18.

We note here that Eq. (2.5) shows that the far field divergence is proportional to the value of the M^2 factor and inversely proportional to the beam waist size. In Fig. 2.17, the mixed mode has a waist radius 10 % larger and an M^2 factor value

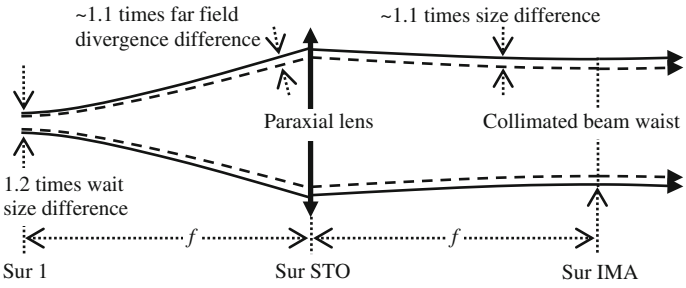

Fig. 2.18 The *solid curves* are for a Gaussian beam with $M^2 = 1.2$, the *dashed curves* are for the embedded Gaussian beam with $M^2 = 1$. The drawing is not to exact proportion for clarity

20 % larger than those of the fundamental mode. Therefore, the mixed mode has 10 % larger far field divergence than that of the fundamental mode.

2.4.2 Focusing a Gaussian Beam

Now we consider using the same *Paraxial* lens to focus a Gaussian beam.

In the table box *Paraxial Gaussian Beam Settings*, keep everything the same, only change the *Waist* value from 0.002 to 1. The Rayleigh range of a 1 mm waist size beam is much larger than the 10 mm focal length. The waist of such a beam at the focal plane of the lens means focusing. Then click the *Update* button at the text box *Paraxial Gaussian Beam Data*, the text box will look like as shown in Fig. 2.19. These numbers can be explained in the same way as in Sect. 2.4.1, we do not repeat it here. We can see that the *Waist* at surface *IMA* is only about 2 μm because it is focusing.

If we want to see the beam data at any other location, we can simply insert new surfaces into the *Lens Data Editor* at these locations. We can also type in other lens

Input Beam Parameters:

Waist size : 1.00000E+000

Surf 1 to waist distance: 0.00000E+000

M Squared : 1.20000E+000

Y-Direction:

Fundamental mode results:

Sur	Size	Waist	Position	Radius	Divergence	Rayleigh
OBJ	1.00000E+000	1.00000E+000	0.00000E+000	Infinity	2.06901E-004	4.83322E+003
1	1.00000E+000	1.00000E+000	0.00000E+000	Infinity	2.06901E-004	4.83322E+003
STO	1.00000E+000	2.06901E-003	-1.00000E+001	-1.00000E+001	9.96687E-002	2.06901E-002
IMA	2.06901E-003	2.06901E-003	0.00000E+000	Infinity	9.96687E-002	2.06901E-002

Mixed Mode results for M2 = 1.2000:

Sur	Size	Waist	Position	Radius	Divergence	Rayleigh
OBJ	1.09545E+000	1.09545E+000	0.00000E+000	1.00000E+010	2.26649E-004	4.83322E+003
1	1.09545E+000	1.09545E+000	0.00000E+000	1.00000E+010	2.26649E-004	4.83322E+003
STO	1.09545E+000	2.26649E-003	-1.00000E+001	-1.00000E+001	1.09182E-001	2.06901E-002
IMA	2.26649E-003	2.26649E-003	0.00000E+000	1.00000E+010	1.09182E-001	2.06901E-002

Fig. 2.19 Zemax modeling of a Paraxial lens focusing a Gaussian beam. Content of the text box *Paraxial Gaussian beam data*

data and beam data to model other propagations. If a real lens is used, the lens aberration must be well corrected. Strong aberrations will deviate a Gaussian beam from basic mode and the result of modeling such a beam is not accurate. We also note that the meaning of signs "+" and "−" can be confusing and require full attention.

References

1. Naqwi, A., et al.: Focusing of diode laser beams: a simple mathematical model. Appl. Opt. **29**, 1780–1785 (1990)
2. Li, Y.: Focusing of diode laser beams: a simple mathematical model: comment. Appl. Opt. **31**, 3392–3393 (1992)
3. Sun, H.: Modeling the near field and far field modes of single spatial mode laser diodes. Opt. Eng. **51**, 044202 (2012)
4. Sun, H.: Thin lens equation for a real laser beam with weak lens aperture truncation. Opt. Eng. **37**, 2906–2913 (1998)
5. Siegmann, A.E.: Lasers, Chapter 16 Wave Optics and Gaussian Beams and Chapter 17 Physical Properties of Gaussian Beams. University Science Books, Mill Valley (1986)
6. Siegman, A.E.: New developments in laser resonators. Proc. SPIE **1224**, 2–14 (1990)
7. Siegman, A.E.: Defining, measuring, and optimizing laser beam quality. Proc. SPIE **1868**, 2 (1993)
8. ISO Standard 11146: Lasers and laser-related equipment—test methods for laser beam widths, divergence angles and beam propagation ratios (2005)
9. Almost any optics text book discusses the thin lens equation
10. Self, S.A.: Focusing of spherical Gaussian beams. Appl. Opt. **22**, 658–661 (1983)
11. Nemoto, S.: Nonparaxial Gaussian beams. Appl. Opt. **29**, 1940–1946 (1990)
12. http://en.wikipedia.org/wiki/Ray_transfer_matrix_analysis
13. Almost any optics text book discusses Snell's law
14. Herloski, R., Marshall, S., Antos, R.: Gaussian beam ray—equivalent modeling and optical design. Appl. Opt. **22**, 1168–1174 (1983)

http://www.springer.com/978-94-017-9782-5

A Practical Guide to Handling Laser Diode Beams

Sun, H.

2015, XII, 136 p. 113 illus., Softcover
ISBN: 978-94-017-9782-5